

See discussions, stats, and author profiles for this publication at: <https://www.researchgate.net/publication/258248687>

Multiplexed Target Detection Using DNA-Binding Dye Chemistry in Droplet Digital PCR

ARTICLE *in* ANALYTICAL CHEMISTRY · NOVEMBER 2013

Impact Factor: 5.64 · DOI: 10.1021/ac403061n · Source: PubMed

CITATIONS

19

READS

426

38 AUTHORS, INCLUDING:



Ryan Koehler

VerdAscend Sciences

24 PUBLICATIONS 793 CITATIONS

[SEE PROFILE](#)



Keith Hamby

Bio-Rad Laboratories

12 PUBLICATIONS 486 CITATIONS

[SEE PROFILE](#)



Viresh Patel

Bio-Rad Laboratories

9 PUBLICATIONS 536 CITATIONS

[SEE PROFILE](#)



John Regan

Bio-Rad Laboratories

24 PUBLICATIONS 476 CITATIONS

[SEE PROFILE](#)

Multiplexed Target Detection Using DNA-Binding Dye Chemistry in Droplet Digital PCR

Geoffrey P. McDermott,^{*,†} Duc Do,[†] Claudia M. Litterst,[†] Dianna Maar,[†] Christopher M. Hindson,[‡] Erin R. Steenblock,[†] Tina C. Legler,[†] Yann Jouvenot,[†] Samuel H. Marrs,[†] Adam Bemis,[†] Pallavi Shah,[†] Josephine Wong,[†] Shenglong Wang,[†] David Sally,[†] Leanne Javier,[†] Theresa Dinio,[†] Chunxiao Han,[†] Timothy P. Brackbill,[†] Shawn P. Hodges,[†] Yunfeng Ling,[†] Niels Klitgord,[†] George J. Carman,[†] Jennifer R. Berman,[†] Ryan T. Koehler,[§] Amy L. Hiddessen,^{||} Pramod Walse,[†] Luc Bousse,[†] Svilen Tzonev,[†] Eli Hefner,[†] Benjamin J. Hindson,[‡] Thomas H. Cauly, III,[†] Keith Hamby,[†] Viresh P. Patel,[†] John F. Regan,[†] Paul W. Wyatt,[†] George A. Karlin-Neumann,[†] David P. Stumbo, and Adam J. Lowe[†]

[†]The Digital Biology Center, Bio-Rad Laboratories, Inc., 5731 West Las Positas Boulevard, Pleasanton, California 94566, United States

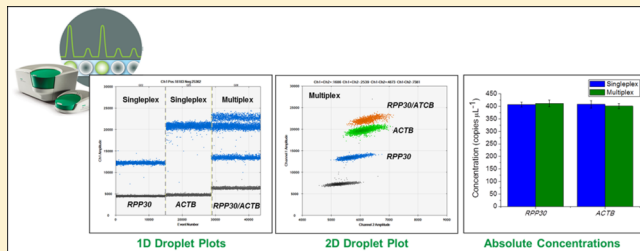
[‡]10X Technologies, Inc., Pleasanton, California 94566, United States

[§]VerdAscend Sciences, West Linn, Oregon, 97068, United States

^{||}Purigen Biosystems, Inc., Alviso, California 95002, United States

S Supporting Information

ABSTRACT: Two years ago, we described the first droplet digital PCR (ddPCR) system aimed at empowering all researchers with a tool that removes the substantial uncertainties associated with using the analogue standard, quantitative real-time PCR (qPCR). This system enabled TaqMan hydrolysis probe-based assays for the absolute quantification of nucleic acids. Due to significant advancements in droplet chemistry and buoyed by the multiple benefits associated with dye-based target detection, we have created a “second generation” ddPCR system compatible with both TaqMan-probe and DNA-binding dye detection chemistries. Herein, we describe the operating characteristics of DNA-binding dye based ddPCR and offer a side-by-side comparison to TaqMan probe detection. By partitioning each sample prior to thermal cycling, we demonstrate that it is now possible to use a DNA-binding dye for the quantification of multiple target species from a single reaction. The increased resolution associated with partitioning also made it possible to visualize and account for signals arising from nonspecific amplification products. We expect that the ability to combine the precision of ddPCR with both DNA-binding dye and TaqMan probe detection chemistries will further enable the research community to answer complex and diverse genetic questions.



INTRODUCTION

For over 25 years, the polymerase chain reaction (PCR) has been the definitive technique for quantifying nucleic acids.^{1,2} The fundamental principles of PCR have remained largely unchanged, but advancements in the development of enzymatic reaction mixtures, thermal cycling instrumentation, and detection systems are continually offering researchers access to previously unattainable genetic information. One of the most significant of these technological progressions has been the advent of digital PCR.^{3,4}

Digital PCR builds on the workflow of quantitative real-time PCR (qPCR), wherein the nucleic acid sample along with primer and/or probe sets are added to a PCR master mix.^{3–8} However, in digital PCR, the sample is first partitioned into hundreds to millions of individual reaction chambers prior to thermal cycling.^{3–8} Recently, we developed a scalable approach

to sample partitioning based on generating monodisperse water-in-oil droplets, coined droplet digital PCR (ddPCR).^{9,10} In this technique, 8 × 20 μL reaction mixtures are simultaneously divided into tens of thousands of surfactant-stabilized droplets using a disposable microfluidic cartridge and a vacuum source (Droplet Generator).^{9,10} The resulting droplets are then transferred into a 96-well plate and thermally cycled.^{9,10} Following end-point amplification, the 96-well plate is loaded into a Droplet Reader that automatically aspirates the emulsion from each well and assigns droplets as being positive (containing template) or negative (no template) based on the

Received: September 22, 2013

Accepted: November 3, 2013

Published: November 3, 2013

their fluorescence emission.^{9,10} The target concentration is then computed using Poisson statistics according to eq 1

$$\lambda = -\ln(1 - p) \quad (1)$$

where p is the fraction of positive droplets and λ represents target copies per droplet (or partition).^{9,10} This digital output affords absolute quantification of nucleic acids without the need for standard curves or endogenous controls. Unlike early realizations of digital PCR, which were restricted to template concentrations in the limiting dilution regime (on average, below one template molecule per partition),^{3,4} the characterized volume of our droplets¹⁰ combined with the number of partitions and Poisson statistics mean that the dynamic range of this technique has been demonstrated across nearly 5 orders of magnitude.¹⁰

Although ddPCR is an inherently powerful tool that has enabled scientific breakthroughs in cancer biomarker discovery, infectious diseases, and genetic alterations,^{9,11–40} current platforms only permit the use of TaqMan probe-based fluorogenic 5' nuclease detection chemistry. This dictates that in addition to primers, researchers must design one or more custom-made fluorescent probes for each target sequence. Some applications such as rare single nucleotide polymorphism detection are enhanced by this added probe specificity; however, for many experiments this unnecessarily increases assay design complexity and costs. An alternative strategy for amplicon detection uses a DNA-binding/intercalating dye that elicits a strong fluorescence signal when associated with double-stranded DNA.^{41–43} Despite the nonspecific nature of amplicon detection, dye-based assays remain popular, as they only require the design and synthesis of primer pairs, can be easily incorporated into previously optimized protocols, and are significantly cheaper than their TaqMan probe-based counterparts.^{41–43}

To date, numerous DNA-binding dyes have been evaluated for use in qPCR; however, SYBR Green has been the most widely utilized.^{1,44–47} This dye is highly fluorescent when bound to double-stranded DNA and produces very little background response.^{45,47} Unfortunately, SYBR Green also possesses a high tendency to inhibit PCR and promote mispriming.^{45,47} Recently, an alternative next-generation DNA-binding dye known as EvaGreen was reported to offer superior performance over other dyes when used in qPCR and for high-resolution melt curve analysis.^{42,43} In a systematic study exploring the binding profile of EvaGreen, Mao et al.⁴³ report that the dye shows no apparent preference for either GC or AT-rich sequences, is stable under both storage and PCR conditions, can be used at significantly higher concentrations than other intercalating dyes (e.g., SYBR Green), binds both single and double-stranded DNA (with a much lower affinity toward single-stranded DNA), and is spectrally similar to the commonly used fluorescent dye, 6-carboxyfluorescein (6-FAM).

Extending the work of our recent publication in this journal (2011, 83, 80604–8610), we herein use a “second generation” ddPCR system to demonstrate the immediate utility of DNA-binding dye based ddPCR. Employing the recently commercialized DNA-binding dye EvaGreen, we show how the fluorescence emission from each droplet directly relates to the mass of DNA encapsulated within. The added resolution associated with partitioning prior to thermal cycling allowed us to exploit this principle to visualize and account for off-target products and enabled the quantification of multiple target

species in a single well of droplets. Furthermore, we show that results obtained with DNA-binding dye based ddPCR are equivalent to their previously reported TaqMan counterparts in precision and dynamic range.

■ RESULTS AND DISCUSSION

The fluorescence emission from DNA-binding dyes is directly proportional to the mass of DNA present in solution, irrespective of whether it is the target sequence or nonspecific product.^{44–47} When using qPCR, this property presents a significant disadvantage as only a single measurement from a bulk solution is obtained.^{1,44–46} In contrast, a single ddPCR well consists of many thousands of fluorescence measurements on an equal number of discrete amplification chambers (droplets). As these droplet partitions contain varying amounts of DNA mass, it is now possible to use a single DNA-binding dye to discriminate multiple sequences from within one sample. As such, a series of experiments were designed to examine the effect of DNA mass on the fluorescent amplitude of droplets with the purpose of determining appropriate operating conditions for EvaGreen-based ddPCR.

Optimal Primer Concentration Range for EvaGreen-Based ddPCR. A dilution series of primers designed to target the Interleukin 4 gene (*IL-4*) was generated from 25–1000 nM in the presence of 0, 0.33, or 3.33 ng μL^{-1} of human genomic DNA (Figure 1). In order to be detected, each droplet must possess a baseline fluorescence signal, even if no reaction occurred inside. For TaqMan-based ddPCR assays, this signal results from the imperfect quenching of fluorogenic probe(s).⁹ However, as can be seen in Figure 1, when employing EvaGreen-based detection the intrinsic fluorescence level of each droplet arises from the amount of primer and background DNA present. For no template control (NTC) wells, the fluorescence intensity of droplets increases proportional to primer concentration as EvaGreen is capable of binding to single-stranded DNA, albeit with a lower affinity (Figure 1a).⁴³ When 3.3 ng μL^{-1} of genomic DNA was present, the amplitude of negative droplets further increased as nontarget containing fragments were partitioned at adequately high levels to enhance their signal above what was originating from primers alone (Figure 1c). To assess the impact of primer and background DNA concentration on the ability to clearly distinguish positive from negative droplets, the degree of separation between these populations was quantified according to eq 2

$$\text{Separation} = \frac{\text{Positive amplitude } \mu - \text{Negative amplitude } \mu}{\text{Positive amplitude } \sigma + \text{Negative amplitude } \sigma} \quad (2)$$

where μ is the mean and σ is the standard deviation of a population's fluorescence amplitude. It was found that the greatest degree of separation between population types occurred when using primer concentrations of 100–200 nM (Figure 1d and e). At concentrations above this value, the amplitude of positive droplets remained constant, but the fluorescence levels of negative droplets increased, resulting in a decrease in separation values. Although a clear distinction between positive and negative droplets was still made when using relatively high primer concentrations (250–1000 nM) and the target concentration was uniform across each condition studied (Figure S1 in the Supporting Information), this reduced degree of separation may affect the ability to draw a

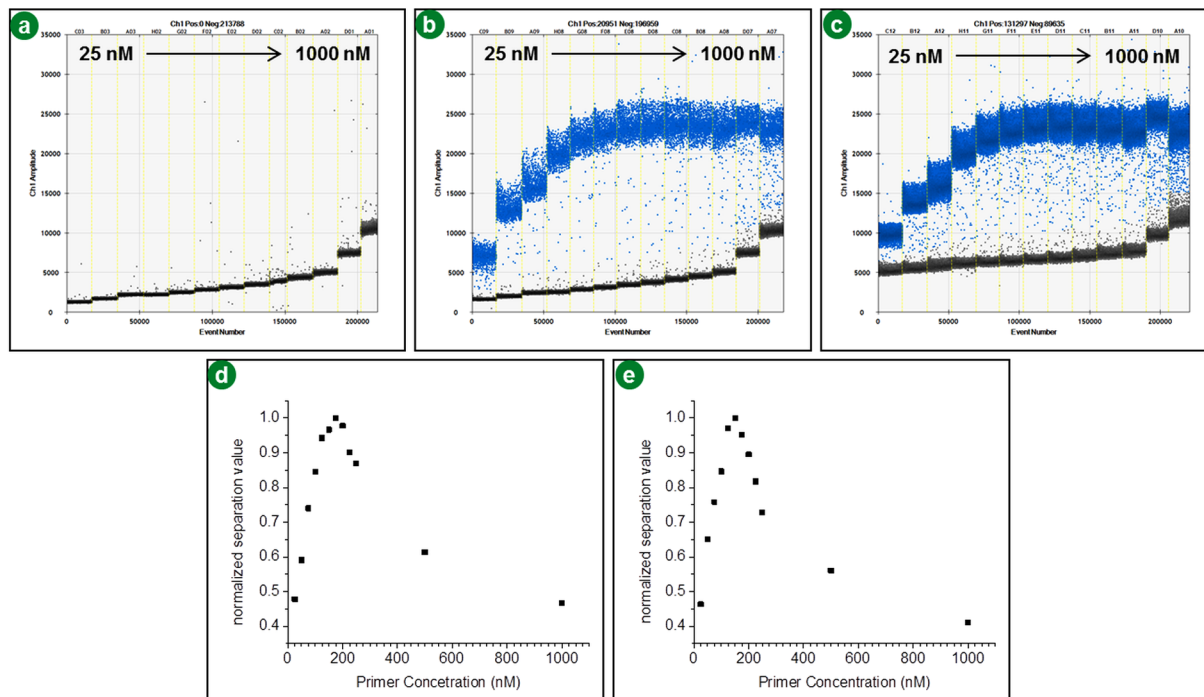


Figure 1. Influence of primer and target concentration on the fluorescence amplitude of droplets in EvaGreen-based ddPCR. Primer concentrations for the *IL-4* target gene were screened from 25–250 nM in 25 nM increments, then 500 and 1000 nM. Resulting 1D Droplet Plots are shown for (a) no template controls and when including (b) 0.33 ng μL^{-1} or (c) 3.33 ng μL^{-1} of purified human genomic DNA in each reaction mixture. The separation between positive and negative populations was calculated according to eq 2 then normalized and plotted against primer concentration for wells that contained (d) 0.33 ng μL^{-1} or (e) 3.33 ng μL^{-1} of template DNA.

threshold between the two population types and obtain an accurate target concentration.

Correlation Between Amplicon Length and Positive Droplet Fluorescence. Since the level of EvaGreen fluorescence is dependent on the mass of DNA present, the influence of amplicon length on the amplitudes of positive droplets was examined. To create a series of assays were designed to target the Ribonuclease P gene (*RPP30*) such that the forward primer sequence remained constant while the reverse was varied to hybridize at increasing distances downstream. This afforded reaction products 62, 99, and 200 base pairs in length, which consequently resulted in positive droplets of increasing fluorescence amplitudes (Figure 2). These observations can be explained by the fact that a greater number of EvaGreen molecules are capable of binding to larger amplicons,⁴³ meaning that once assays of similar reaction efficiency are cycled to the end point, a more intense fluorescence response is obtained for longer PCR products than shorter ones. This principle was employed in experiments that are described later in this text to achieve the multiplexed detection of two separate targets in just one well of droplets (Figures 4, 5, 6, and S6). Moreover, being able to differentiate amplicon length based on fluorescence amplitude can provide important information when preparing next-generation sequencing libraries as described in a recent report.⁴⁸

Effect of Input DNA Concentration on Dynamic Range. To further evaluate factors influencing the dynamic range of the EvaGreen detection system, two separate EvaGreen assays were constructed, each containing a dilution series of digested human genomic DNA from 8.2 pg μL^{-1} to 16.5 ng μL^{-1} (2.5–5000 copies μL^{-1} of each target) per reaction. The targeted gene for each reaction was either *RPP30*

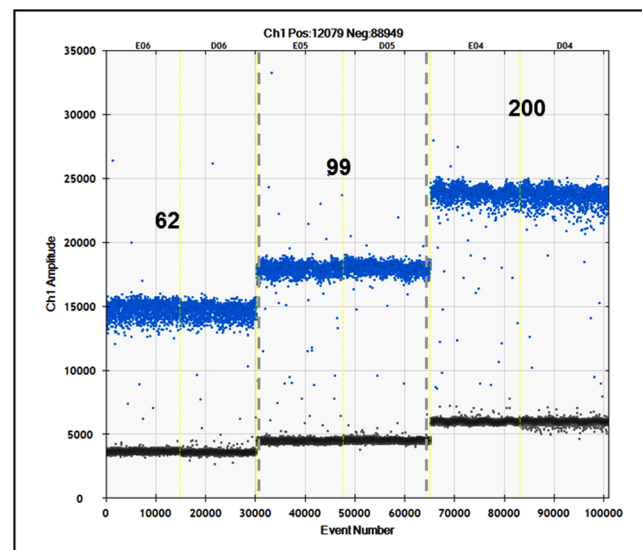


Figure 2. Effect of amplicon length on the fluorescence amplitude of positive droplets in EvaGreen-based ddPCR. 1D Droplet Plots for three *RPP30* assays where the forward primer sequence was kept constant but the reverse was varied to produce differing sized amplicons. Numbers above the positive droplet populations indicate the predicted base-pair length of each reaction product. The fluorescence amplitude of positive droplets increased with amplicon length as multiple dye molecules bind the same PCR product.

or β -actin (*ACTB*), which resulted in the production of 62 and 137 base-pair amplicons respectively. Following amplification in the EvaGreen-containing reaction mixtures, positive droplets encapsulating the longer *ACTB* product were of higher fluorescence amplitude in comparison to those of the *RPP30*

assay (Figure S2 in the Supporting Information). As the same primer concentration was used for both assays, this result was due to the 105 base-pair difference in amplicon length. The input concentration of target sequence had little impact on the amplitude of positive droplets but did significantly alter the fluorescence intensity of negative droplets as it is a function of the primer/background DNA levels (Figure S2). The increase in amplitude associated with background genomic DNA only became problematic at concentrations of $9 \text{ ng } \mu\text{L}^{-1}$ and higher for the *RPP30* assay as it impacted the ability to clearly distinguish positive from negative signals (Figure S2). To overcome this poor separation between populations, the experiment was repeated with double the original primer concentration ($100 \rightarrow 200 \text{ nM}$). This yielded more amplification product (DNA mass) and thus a higher overall fluorescence signal for each positive droplet, making it possible to unambiguously quantify the target to the highest concentration of DNA screened ($16.5 \text{ ng } \mu\text{L}^{-1}$). The ddPCR responses obtained for each species were highly linear over the 4 orders of magnitude examined (Figure S2). Since dynamic range is primarily a function of the number of partitions (droplets) available,⁴⁹ as expected, these results were equivalent to the performance of other previously reported TaqMan-based ddPCR assays.^{9,10}

Comparison of EvaGreen and TaqMan Based ddPCR.

To further demonstrate the ability to obtain an absolute digital measurement independent of the type of detection chemistry employed, both EvaGreen and TaqMan-based assays were used for the quantification of five genes using 10 separate targeted assays. The same primer pairs were used for both EvaGreen and TaqMan versions of each reaction, which were performed in duplicate and accompanied by a NTC. Across these assays, the input amount of human genomic DNA remained constant ($1.65 \text{ ng } \mu\text{L}^{-1}$), amplicon length was varied from 88 to 508 base pairs, and GC content ranged from 34 to 62% (see Table S-1 in the Supporting Information for assay information). Overall, the measured concentrations were found to be analogues (within $\pm 2.5\%$) when employing either EvaGreen or TaqMan forms of each assay (Figure 3). Furthermore, the separation between positive and negative populations was comparable between the two detection chemistry types with exception of the *B2M* (2), *IL-4* (1), and *EEF2* assays (Figure S3 in the Supporting Information). In these examples, even though equivalent concentrations were obtained, the ability to distinguish positive from negative populations was more difficult when using TaqMan probes in comparison to the EvaGreen dye. This can be attributed to the long amplicon lengths that result from these assays (458–508 base pairs) to which multiple EvaGreen molecules can bind and elicit a strong signal, but the hydrolysis of TaqMan probes is reduced, causing low fluorescence signals. Furthermore, the concentrations obtained for the *B2M* (2), *IL-4* (1) and *EEF2* targets were 10–15% lower than expected based on the amount of input DNA into each reaction (Figure S3). For all other targets, intra-assay concentrations were in good agreement, differing by $\pm 5\%$ from each other and within $\pm 4\%$ of the expected template copy number.

Detection of Nonspecific Amplification Products. A limitation of using DNA-binding dyes in qPCR is their ability to bind to any double-stranded DNA sequence, which means that both specific and nonspecific PCR products contribute to the overall fluorescence response.^{1,44–46} However, in digital PCR, many hundreds to millions of individual fluorescence measure-

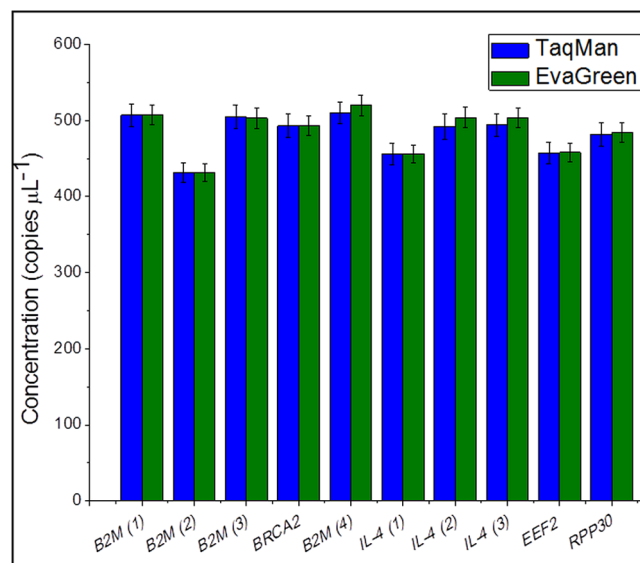


Figure 3. Concentration measurements for 10 target sequences on five separate genes using TaqMan (blue) and EvaGreen (green) based ddPCR. Error bars indicate the Poisson 95% confidence interval.

ments are made for each sample. As such, EvaGreen-based ddPCR was used to examine the effects of nonspecific product formation on the quantification of three separate targets. The first assay was designed to measure the *NCoA-1* gene, which is responsible for encoding the nuclear receptor coactivator 1 protein.⁵⁰ In this example, sense and antisense primer sequences of high homology were employed to purposely induce the formation of primer-dimers. To further increase the levels of this amplification artifact, temperature gradient PCR was also employed. Examination of NTCs revealed the presence of primer-dimers (Figure 4a), with their concentration increasing from 0.7 to 20 copies μL^{-1} as the annealing temperature was decreased from 66 to 55 °C (Figure S4 in the Supporting Information). As previously shown (Figure 2), EvaGreen signal intensity is related to amplicon length, so when DNA was included in the reaction mixture, the relatively short primer-dimer sequences resulted in droplets of lower fluorescence amplitude in comparison to those containing the targeted species (Figure 4a). Therefore, a clear threshold was drawn above the primer-dimer containing droplets and below the true positive droplet types (Figure 4a), making the resulting concentration unaffected by the presence of this nonspecific product (Figure 4b). The remaining two assays were designed to target the *GAPDH* and *ACTB* genes respectively, and gradient PCR was used once again to induce the formation of spurious reaction products (Figure 4c and e). In both examples, almost no positive droplets were observed in the NTC wells since primer-dimers were avoided during assay design (Figure 4c and e). However, in the presence of template DNA, off-target reaction species were produced in both assays at the lower annealing temperatures (55–57.2 °C). This resulted in the appearance of droplets above and below the primary population of true positives (Figure 4c and e) and was accompanied by a noticeable spike in the concentrations measured (Figure 4d and g). Although these off-target amplification products were easily visualized, in the case of the *GAPDH* assay their effect on target concentration could not be corrected for. However, when results of the *ACTB* assay were viewed in a 2D Droplet Plot, droplets containing the off-

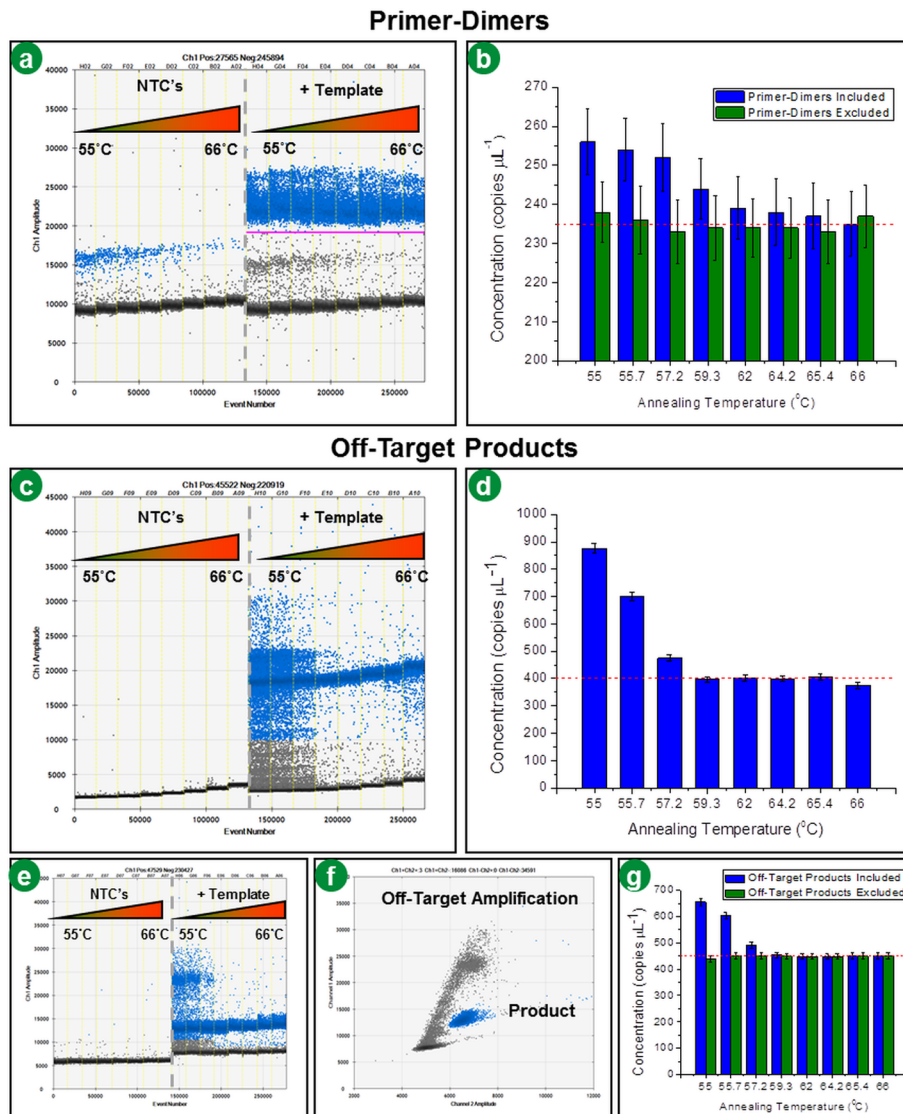


Figure 4. Nonspecific product formation in EvaGreen-based ddPCR. (a) 1D Droplet Plots of an NCoA-1 assay that formed primer-dimer products, as evident in NTC wells. (b) Concentration measurements from the NCoA-1 assay where a primer-dimer product was included (blue) and excluded (green) from the positive droplet population using manually drawn thresholds. (c) 1D Droplet Plots of a GAPDH assay that produced off-target amplification at lower annealing temperatures. (d) Concentration measurements from the GAPDH assay. (e) 1D Droplet Plots of an ACTB assay that produced off-target amplification at lower annealing temperatures. (f) 2D Droplet Plot of results obtained at annealing temperatures of 55 to 57.2 °C for the ACTB assay. Off-target product(s) produced a distinct cluster, separate from the population of droplets containing desired product. (g) Concentration measurements from the ACTB assay where off-target product(s) was included (blue) and excluded (green) from the positive droplet population using manually drawn thresholds. Sloping triangles and temperatures displayed on 1D temporal Droplet Plots in a, c, and e represent the gradient anneal-extend step of the thermal cycling protocol employed. Error bars in b, d, and g indicate the Poisson 95% confidence interval.

target product(s) were of different fluorescence amplitudes than those of the true positives (Figure 4f). By drawing manual thresholds in a way that excluded this off-target population, precise quantification of the desired sequence was achieved (Figure 4g). Although in these examples the fluorescent amplitude of droplets was utilized to discriminate nonspecific products, digital PCR MIQE guidelines⁵¹ such as in silico primer specificity screens, avoidance of primer-dimers, and secondary structure along with the consideration of pseudogenes are still necessary during assay design and remain good practice. In addition, inclusions of NTCs are essential because they provide a method to visualize and quantify undesired amplification products and allow for the identification of droplet subpopulations as either being primer-dimer or off-target amplification products.

Single Color Multiplexing Using EvaGreen-Based ddPCR. When performing intercalating dye reactions in qPCR, the quantification of multiple amplification products from one reaction mixture is unachievable as only a single fluorescent measurement is made in each detection channel. However, with ddPCR, variations in the fluorescence signal intensity of EvaGreen due to the mass of DNA present in each droplet can actually be utilized for multiplexed detection. This can reliably be achieved by adjusting the following experimental parameters individually or in combination, since each impacts the amount of reaction product generated and thus the fluorescence intensity of positive droplets: amplicon length, primer concentration, and annealing temperature. To demonstrate these principles, two EvaGreen-based multiplex ddPCR experiments were conducted. In each example, individual assays

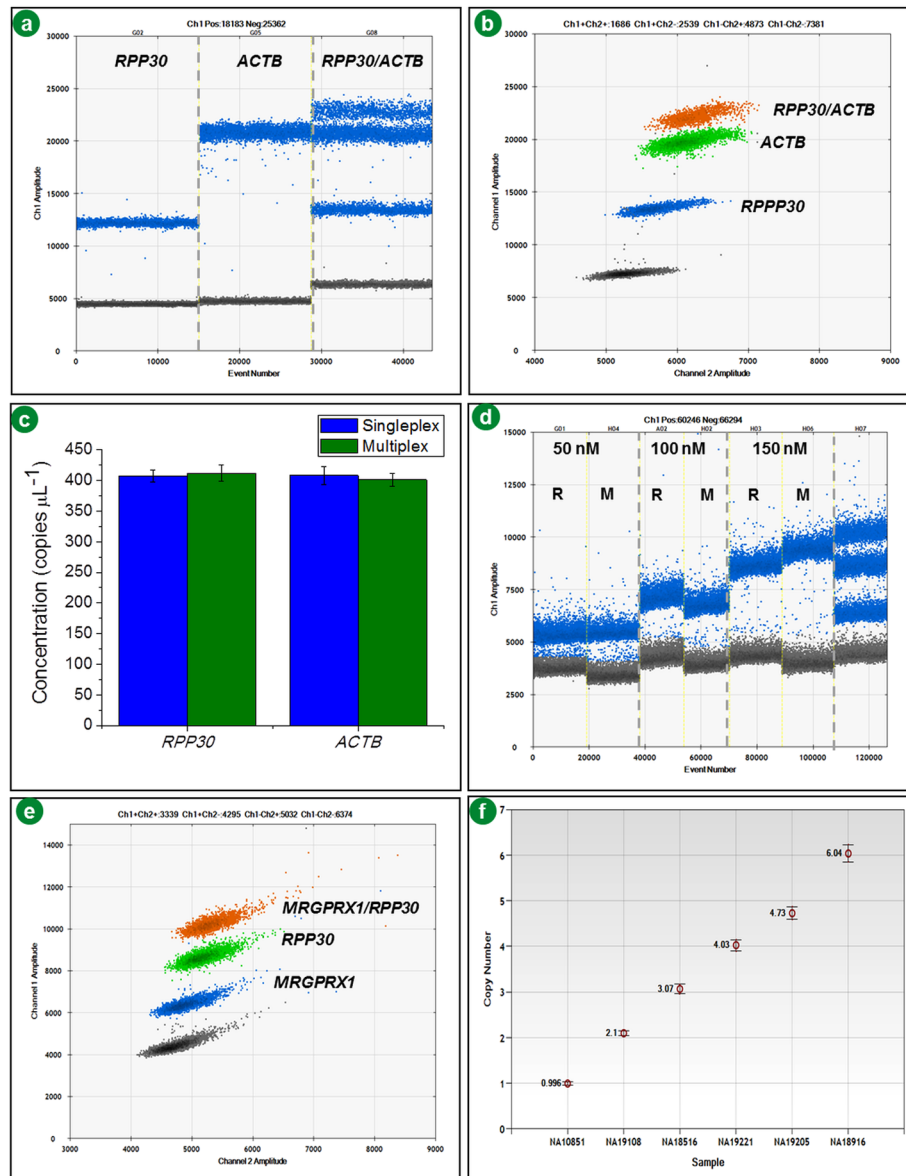


Figure 5. Multiplexed target detection using EvaGreen-based ddPCR. (a) 1D Droplet Plots from *RPP30* and *ACTB* assays which resulted in 62 and 137 base-pair reaction products, respectively. Multiplexed detection (based on differences in amplicon lengths) of both genes was achieved by combining these assays into a single reaction. (b) 2D Droplet Plot of the *RPP30/ACTB* multiplex assay. Manual thresholds were drawn to assign clusters. (c) Concentration measurements of the *RPP30/ACTB* targets from singleplex and multiplex reactions in (a and b). Error bars indicate the Poisson 95% confidence intervals. (d) 1D Droplet Plots from *RPP30* (R) and *MRGPRX1* (M) assays, with concentrations representing primer levels. Multiplexed detection (based on differing primer concentrations) of both genes was achieved by combining the *RPP30* and *MRGPRX1* assays into a single reaction and employing primer concentrations of 150 and 50 nM, respectively. (e) 2D Droplet Plot of the *RPP30/MRGPRX1* multiplex assay. Manual thresholds were drawn to assign clusters. (f) Measurements of *MRGPRX1* copy number states in HapMap samples. Each data point was obtained from a single well of droplets using the aforementioned *RPP30/MRGPRX1* EvaGreen-based multiplexed reaction. Error bars indicate the Poisson 95% confidence intervals.

were included to provide a reference concentration for each target and ensure that there were no spurious amplification products. To begin with, the two previously described *RPP30* and *ACTB* assays from were combined into one ddPCR reaction to detect both targets based on the difference in their amplicon lengths (Figure 5a and b). This resulted in four distinct droplet populations of independent fluorescence amplitudes that were evident in both the 1D and the 2D Droplet Plots (Figure 5a and b). The lowermost of these was the nontarget containing negative droplets, while the next two bands of increased fluorescence were comprised of droplets that possessed only one target type . As the *ACTB* amplification

product is longer than that of *RPP30* (137 compared to 62 base pairs), droplets encapsulating this amplicon were of higher fluorescence amplitude. The final population of droplets (double positives) contained both *ACTB* and *RPP30* target sequences and consequently had the greatest fluorescence amplitude. Quantification of both genes was achieved by viewing droplets in a 2D Droplet Plot, as this made it possible to use 2D clustering tools to assign four different populations (double negative, two single positive clusters, and a double positive cluster) similar to a two color multiplex ddPCR assay using TaqMan reagents (Figure 5b). The resulting concentration of each species was then artificially assigned to either the

FAM or VIC channel and was shown to directly match ($\pm 1.8\%$) the values obtained when analyzing these targets individually (Figure 5c).

The second example of EvaGreen-based multiplexing was achieved by varying primer concentration to generate differing levels of amplified DNA mass/positive droplet fluorescence for each target sequence. Initially, individual assays were constructed for the *MRGPRX1* and *RPP30* genes with primer concentrations ranging from 50 to 150 nM (Figure 5d). Since there was only an eight base-pair difference in the length of amplicon produced from the *MRGPRX1* and *RPP30* targets (70 versus 62 base pairs, respectively), positive droplets in each assay were of comparable fluorescence amplitude when employing the same primer concentration (Figure 5d). However, as primer levels were increased from 50 to 150 nM, there was an associated rise in the fluorescence amplitude of positive droplets for both assay types. Therefore, successful multiplexing was achieved by tripling the concentration of the *RPP30* primers (150 nM) in comparison to those of *MRGPRX1* (50 nM). In this regime, more of the *RPP30* amplicon was produced, which meant higher fluorescence intensities for these droplets types (Figure 5e). Once more, 2D clustering tools were used to assign four different populations and the resulting concentrations obtained for each target from multiplexed wells were similar to those calculated in parallel individual reactions (Figure S5 in the Supporting Information). To demonstrate the immediate analytical utility of multiplexed detection using EvaGreen-based ddPCR, the copy number states of the *MRGPRX1* gene were assessed in six different HapMap samples (Figure 5f). In this example, different primer concentrations were used for the *MRGPRX1* target (50 nM) and *RPP30* reference gene (150 nM), which resulted in unambiguous cluster separation (Figure S6 in the Supporting Information). This assay design made it possible to completely resolve *MRGPRX1* integer copy numbers from 1 to 6 with 95% confidence using just a single well of droplets for each sample (Figure 5f).

An alternative strategy for multiplexed detection was also developed where TaqMan-probe and DNA-binding dye based chemistries were combined in the same reaction. To demonstrate this principle, we employed primer-based allelic detection of the *BRAF V600E* wild-type locus in combination with a VIC probe-based *RPP30* reference assay in one well of droplets. Initially, these reactions were performed individually on purified DNA extracted from a human female cell line (Coriell, NA19205). Primer concentrations of 100 nM were employed and the *RPP30* assay also included 100 nM of a VIC fluorophore labeled probe sequence. When comparing the resulting 1D Droplet Plots side-by-side (Figure 6a), positive droplets from the *BRAF V600E* assay were of higher fluorescence amplitude in comparison to those of the *RPP30* due to their differing amplicon lengths (104 versus 62 base pairs, respectively). When the two assays were combined into a single reaction and results viewed in a 1D Droplet Plot, this difference in fluorescence amplitude was not large enough to fully resolve the two single positive populations (Figure 6a). However, when using a 2D Droplet Plot to display the same data, four distinct clusters were observed (Figure 6b). As successful amplification of the *RPP30* target was detected by EvaGreen and probe-based chemistry, clusters containing this species produced a stronger signal in the VIC channel. This caused these populations to shift in the right/VIC direction relative to the cluster of droplets containing only EvaGreen and

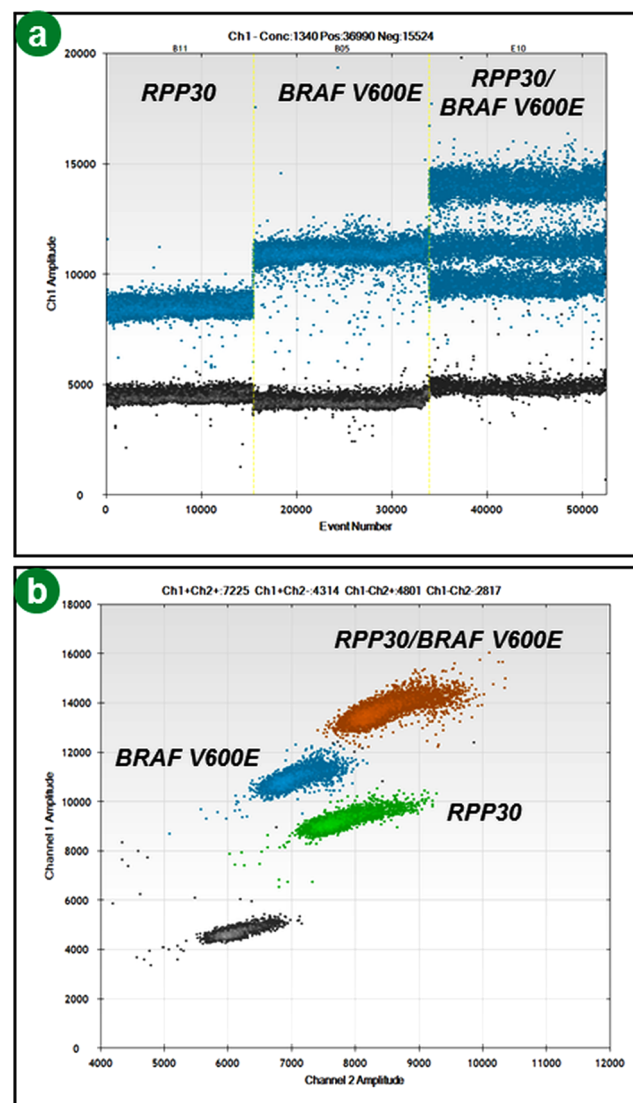


Figure 6. Multiplexed target detection using EvaGreen and TaqMan Probe based chemistry in a single reaction. (a) 1D Droplet Plots showing results from a *RPP30* assay which included 100 nM of a VIC-labeled probe sequence in an EvaGreen-based reaction mixture; *BRAF V600E* assay prepared in EvaGreen-based Supermix; and multiplexed detection of both *RPP30* and *BRAF V600E* targets achieved by combining the two aforementioned assays in one reaction. (b) 2D Droplet Plot of the *RPP30/BRAF V600E* multiplex assay. Manual thresholds were drawn to assign clusters.

the amplified *BRAF V600E* product, allowing for absolute quantification of both target species from the same reaction. The concentrations obtained directly matched those from the singleplex version of each assay (Figure S7 in the Supporting Information). Furthermore, the heterozygous *BRAF V600E* status and gene copy number of the sample tested was consistent with its genetic identity.⁹

Summary. There are several inherent drawbacks associated with using DNA-binding dyes for amplicon detection in the analogue-standard qPCR. Of primary concern is their ability to indiscriminately bind any double-stranded DNA present which makes the fluorescence emission intensity directly related to DNA mass. However, digital PCR addresses this issue by partitioning a sample into thousands of individual discrete reaction vessels prior to thermal cycling. This transforms what

used to be a fundamental limitation of DNA-binding dyes into an essential property that presents many benefits. EvaGreen is capable of binding single-stranded primer sequences and background DNA to allow detection of negative droplets. To this end, primer concentrations of 100–250 nM were found to provide a sufficient fluorescence signal while delivering maximum separation between negative and positive droplets. Furthermore, when levels of 9 ng μL^{-1} and higher of human genomic DNA were reached, the fluorescence levels of negative droplets substantially increased, but quantification of the target species was still possible. Nonspecific products and primer-dimers can also contribute to the fluorescence emission of negative droplets. However, unlike qPCR, in some cases it was possible to draw thresholds and assign droplets as being positive or negative in a way that excludes the droplet population(s) arising from nonspecific product(s) to obtain accurate quantification of the desired sequence. Logically, for target-containing positive droplets, it is the mass of the reaction product encapsulated within that determines their fluorescence intensity. However, the act of partitioning provided the unprecedented resolution to enable the use of just one DNA-binding dye for the multiplexed detection of separate reaction products in a single fluorescence channel. Since ddPCR is inherently more tolerant of PCR efficiency,⁹ by adjusting amplicon length or primer concentrations, one target species produces a higher amount of amplified DNA mass per droplet than the other. As a result, multiple positive droplet clusters were observed and assigned to each target of interest for quantification. Moreover, a VIC-labeled probe was included in a dye-based assay to also achieve multiplexed detection. The linear dynamic range of EvaGreen-based ddPCR was demonstrated to be equivalent to the 4 orders of magnitude observed with TaqMan ddPCR chemistry. When utilizing the same primers, EvaGreen and TaqMan DNA-detection chemistries performed comparably for the quantification of 10 separate targets. Overall, the added dimensionality associated with using a DNA-binding dye in ddPCR along with the practicality of only having to design primer pairs will allow researchers to explore new genetic frontiers with the inherent power of digital PCR.

■ EXPERIMENTAL SECTION

Droplet Digital PCR Workflow and Data Analysis. The ddPCR workflow was similar to what has been previously described.^{9,10} A 20 μL aliquot was taken from each of the assembled ddPCR mixtures and pipetted into each sample well of an eight-channel disposable droplet generator cartridge (Bio-Rad, Hercules, CA, USA). A 70 μL volume of Droplet Generation Oil for EvaGreen (Bio-Rad) or Droplet Generation Oil for Probes (Bio-Rad) was then loaded into each of the eight oil wells. The cartridge was placed into the droplet generator (Bio-Rad) where a vacuum was applied to the outlet wells to simultaneously partition each 20 μL sample into nanoliter sized droplets. After \sim 1.5 min, the cartridge was removed from the generator, and the droplets that had collected in each of the independent outlet wells were transferred with a multichannel pipet to a 96-well polypropylene plate (Eppendorf, Hamburg, Germany). The plate was heat-sealed with foil using a PX1 PCR Plate Sealer (Bio-Rad) and placed in a conventional thermal cycler (C1000 Touch, Bio-Rad). Unless otherwise stated, thermal cycling conditions for all EvaGreen assays consisted of an activation period (5 min at 95 °C) followed by 40 cycles of a two-step thermal profile comprising of a

denaturation step (30 s at 95 °C) and a combined annealing-extension step (60 s at 60 °C). A dye-stabilization step was also included at the end of each EvaGreen thermal cycling protocol (4 °C for 5 min then, 95 °C for 5 min, and finally a 4 °C indefinite hold). Thermal cycling conditions for all TaqMan assays consisted of a 10 min activation period (95 °C) followed by 40 cycles of a two-step thermal profile comprising a denaturation step (30 s at 94 °C) and a combined annealing-extension step (60 s at 60 °C). An enzymatic heat kill step was included at the end of each TaqMan thermal cycling protocol (10 min at 98 °C, then a 4 °C indefinite hold). A 2 °C per second ramp rate was applied for all thermal cycling steps. After PCR, the 96-well plate was loaded into the QX200 Droplet Reader (Bio-Rad), and the appropriate assay information was entered into the analysis software package provided (QuantaSoft, Bio-Rad). Droplets were automatically aspirated from each well and streamed single-file past a two-color fluorescence detector and finally to waste. The quality of all droplets was analyzed and rare outliers (e.g., doublets, triplets) were gated based on detector peak width. Analysis of the ddPCR data was performed with QuantaSoft analysis software (Bio-Rad) that accompanied the QX200 Droplet Reader. All assay information is located in the experimental section of the Supporting Information.

■ ASSOCIATED CONTENT

S Supporting Information

Additional information as noted in the text. This material is available free of charge via the Internet at <http://pubs.acs.org>.

■ AUTHOR INFORMATION

Corresponding Author

*E-mail: geoff_mcdermott@bio-rad.com.

Notes

The authors declare the following competing financial interest(s): Bio-Rad Laboratories, Inc., markets and sells the QX200 Droplet Digital PCR System. C.M.H., A.L.H., R.T.K., and B.J.H. were formerly employees of Bio-Rad Laboratories, Inc., including during periods when the work was done.

■ ACKNOWLEDGMENTS

The authors would like to acknowledge the team of professionals at Bio-Rad Laboratories Inc. (past and present) who have contributed to the QX200 Droplet Digital PCR System. We also thank J. M. Terry for advice during the preparation of this manuscript.

■ REFERENCES

- (1) Heid, C. A.; Stevens, J.; Livak, K. J.; Williams, P. M. *Genome Res.* **1996**, *6*, 986–994.
- (2) Kubista, M.; Andrade, J. M.; Bengtsson, M.; Forootan, A.; Jonák, J.; Lind, K.; Sindelka, R.; Sjöback, R.; Sjögren, B.; Strömbom, L. *Mol. Aspects Med.* **2006**, *27*, 95–125.
- (3) Sykes, P.; Neoh, S.; Brisco, M.; Hughes, E.; Condon, J.; Morley, A. *BioTechniques* **1992**, *13*, 444–449.
- (4) Vogelstein, B.; Kinzler, K. W. *Proc. Natl. Acad. Sci. U. S. A.* **1999**, *96*, 9236–9241.
- (5) Fan, H. C.; Quake, S. R. *Anal. Chem.* **2007**, *79*, 7576–7579.
- (6) Ottesen, E. A.; Hong, J. W.; Quake, S. R.; Leadbetter, J. R. *Science* **2006**, *314*, 1464–1467.
- (7) Warren, L.; Bryder, D.; Weissman, I. L.; Quake, S. R. *Proc. Natl. Acad. Sci. U. S. A.* **2006**, *103*, 17807–17812.

- (8) Morrison, T.; Hurley, J.; Garcia, J.; Yoder, K.; Katz, A.; Roberts, D.; Cho, J.; Kanigan, T.; Ilyin, S. E.; Horowitz, D. *Nucleic Acids Res.* **2006**, *34*, e123–e123.
- (9) Hindson, B. J.; Ness, K. D.; Masquelier, D. A.; Belgrader, P.; Heredia, N. J.; Makarewicz, A. J.; Bright, I. J.; Lucero, M. Y.; Hiddessen, A. L.; Legler, T. C. *Anal. Chem.* **2011**, *83*, 8604–8610.
- (10) Pinheiro, L. B.; Coleman, V. A.; Hindson, C. M.; Herrmann, J.; Hindson, B. J.; Bhat, S.; Emslie, K. R. *Anal. Chem.* **2011**, *84*, 1003–1011.
- (11) Abyzov, A.; Mariani, J.; Palejev, D.; Zhang, Y.; Haney, M. S.; Tomasini, L.; Ferrandino, A. F.; Belmaker, L. A. R.; Szekely, A.; Wilson, M. *Nature* **2012**, *492*, 438–442.
- (12) Agapova, S.; Stephenson, K.; Manary, M.; Weisz, A.; Tarr, P. I.; Mkakosya, R.; Maleta, K.; Shulman, R. J.; Manary, M.; Shaikh, N. J. *Pediatr. Gastroenterol. Nutr.* **2013**, *56*, 66–71.
- (13) Baker, M. *Nat. Methods* **2012**, *9*, 541.
- (14) Belgrader, P.; Tanner, S. C.; Regan, J. F.; Koehler, R.; Hindson, B. J.; Brown, A. S. *Clin. Chem.* **2013**, *59*, 991–994.
- (15) Boettger, L. M.; Handsaker, R. E.; Zody, M. C.; McCarroll, S. A. *Nat. Genet.* **2012**, *44*, 881–885.
- (16) Chen, R.; Mias, G. I.; Li-Pook-Than, J.; Jiang, L.; Lam, H. Y.; Chen, R.; Miriami, E.; Karczewski, K. J.; Hariharan, M.; Dewey, F. E. *Cell* **2012**, *148*, 1293–1307.
- (17) Criscione, F.; Qi, Y.; Saunders, R.; Hall, B.; Tu, Z. *Insect Mol. Biol.* **2013**, *22*, 433–441.
- (18) Davidson, L. A.; Goldsby, J. S.; Callaway, E. S.; Shah, M. S.; Barker, N.; Chapkin, R. S. *Biochim. Biophys. Acta, Mol. Basis Dis.* **2012**, *1882*, 1600–1607.
- (19) Day, E.; Dear, P. H.; McCaughan, F. *Methods* **2012**, *59*, 101–107.
- (20) Dodd, D. W.; Gagnon, K. T.; Corey, D. R. *Nucleic Acid Ther.* **2013**, *23*, 188–194.
- (21) Eriksson, S.; Graf, E. H.; Dahl, V.; Strain, M. C.; Yukl, S. A.; Lysenko, E. S.; Bosch, R. J.; Lai, J.; Chioma, S.; Emad, F. *PLoS Pathog.* **2013**, *9*, e1003174.
- (22) Gevensleben, H.; Garcia-Murillas, I.; Graeser, M. K.; Schiavon, G.; Osin, P.; Parton, M.; Smith, I. E.; Ashworth, A.; Turner, N. C. *Clin. Cancer Res.* **2013**, *19*, 3276–3284.
- (23) Nadauld, L.; Regan, J. F.; Miotke, L.; Pai, R. K.; Longacre, T. A.; Kwok, S. S.; Saxonov, S.; Ford, J. M.; Ji, H. P. *Sci. Transl. Med.* **2012**, *2*.
- (24) Hayden, R.; Gu, Z.; Ingersoll, J.; Abdul-Ali, D.; Shi, L.; Pounds, S.; Caliendo, A. *J. Clin. Microbiol.* **2013**, *51*, 540–546.
- (25) Henrich, T. J.; Gallien, S.; Li, J. Z.; Pereyra, F.; Kuritzkes, D. R. *J. Virol. Methods* **2012**, *186*, 68–72.
- (26) Heredia, N. J.; Belgrader, P.; Wang, S.; Koehler, R.; Regan, J.; Cosman, A. M.; Saxonov, S.; Hindson, B.; Tanner, S. C.; Brown, A. S. *Methods* **2012**, *59*, S20–S23.
- (27) Kelley, K.; Cosman, A.; Belgrader, P.; Chapman, B.; Sullivan, D. *C. J. Clin. Microbiol.* **2013**, *51*, 2033–2039.
- (28) Last, A.; Molina-Gonzalez, S.; Cassama, E.; Butcher, R.; Nabucassa, M.; McCarthy, E.; Burr, S. E.; Mabey, D. C.; Bailey, R. L.; Holland, M. J. *J. Clin. Microbiol.* **2013**, *51*, 2195–2203.
- (29) Liu, B.; Escalera, J.; Balakrishna, S.; Fan, L.; Caceres, A. I.; Robinson, E.; Sui, A.; McKay, M. C.; McAlexander, M. A.; Herrick, C. A. *FASEB J.* **2013**, *27*, 3549–3563.
- (30) Miyake, K.; Yang, C.; Minakuchi, Y.; Ohori, K.; Soutome, M.; Hirasawa, T.; Kazuki, Y.; Adachi, N.; Suzuki, S.; Itoh, M. *PLoS One* **2013**, *8*, e66729.
- (31) Morisset, D.; Štebih, D.; Milavec, M.; Gruden, K.; Žel, J. *PLoS One* **2013**, *8*, e62583.
- (32) Podlesniy, P.; Figueiro-Silva, J.; Llado, A.; Antonell, A.; Sanchez-Valle, R.; Alcolea, D.; Lleo, A.; Molinuevo, J. L.; Serra, N.; Trullas, R. *Ann. Neurol.* **2013**, DOI: 10.1002/ana.23955.
- (33) Porensky, P. N.; Mitrpan, C.; McGovern, V. L.; Bevan, A. K.; Foust, K. D.; Kaspar, B. K.; Wilton, S. D.; Burghes, A. H. *Hum. Mol. Genet.* **2012**, *21*, 1625–1638.
- (34) Sedlak, R. H.; Jerome, K. R. *Diagn. Microbiol. Infect. Dis.* **2012**, *75*, 1–4.
- (35) Srivastava, A. K.; Renusch, S. R.; Naiman, N. E.; Gu, S.; Sneh, A.; Arnold, W. D.; Sahenk, Z.; Kolb, S. J. *Neurobiol. Dis.* **2012**, *47*, 163–173.
- (36) Strain, M. C.; Lada, S. M.; Luong, T.; Rought, S. E.; Gianella, S.; Terry, V. H.; Spina, C. A.; Woelk, C. H.; Richman, D. D. *PLoS One* **2013**, *8*, e55943.
- (37) Strain, M. C.; Richman, D. D. *Curr. Opin. HIV AIDS* **2013**, *8*, 106–110.
- (38) Suehiro, Y.; Okada, T.; Shikamoto, N.; Zhan, Y.; Sakai, K.; Okayama, N.; Nishioka, M.; Furuya, T.; Oga, A.; Kawauchi, S. *Tumor Biol.* **2013**, *33*, 1–6.
- (39) Ward, D. S.; Eva, M.; Maja, K.; Pawel, B.; Chris, V.; Dirk, V.; Linos, V. *Anal. Biochem.* **2013**, *439*, 201–203.
- (40) Yeh, I.; von Deimling, A.; Bastian, B. C. *J. Natl. Cancer Inst.* **2013**, *105*, 917–919.
- (41) Higuchi, R.; Dollinger, G.; Walsh, P. S.; Griffith, R. *Biotechnology* **1992**, *10*, 413–417.
- (42) Eischeid, A. *BMC Res. Notes* **2011**, *4*, 263.
- (43) Mao, F.; Leung, W.-Y.; Xin, X. *BMC Biotechnol.* **2007**, *7*, 76.
- (44) Bengtsson, M.; Karlsson, H. J.; Westman, G.; Kubista, M. *Nucleic Acids Res.* **2003**, *31*, e45–e45.
- (45) Wittwer, C. T.; Herrmann, M. G.; Moss, A. A.; Rasmussen, R. P. *BioTechniques* **1997**, *22*, 130–139.
- (46) Bustein, S. A.; Nolan, T. *J. Biomol. Tech.* **2004**, *15*, 155–166.
- (47) Zipper, H.; Brunner, H.; Bernhagen, J.; Vitzthum, F. *Nucleic Acids Res.* **2004**, *32*, e103–e103.
- (48) Laurie, M. T.; Bertout, J. A.; Taylor, S. D.; Burton, J. N.; Shendure, J. A.; Bielas, J. H. *BioTechniques* **2013**, *55*, 61–67.
- (49) Dube, S.; Qin, J.; Ramakrishnan, R. *PLoS One* **2008**, *3*, e2876.
- (50) Beato, M.; Herrlich, P.; Schütz, G. *Cell* **1995**, *83*, 851–857.
- (51) Huggett, J. F.; Foy, C. A.; Benes, V.; Emslie, K.; Garson, J. A.; Haynes, R.; Hellmann, J.; Kubista, M.; Mueller, R. D.; Nolan, T. *Clin. Chem.* **2013**, *59*, 892–902.